Paper

Three-branch waveguides for even division of optical power on a new design concept

Non-member Tetsuro Yabu (Osaka Prefecture University)
Non-member Masahiro Geshiro (Osaka Prefecture University)
Member Shinnosuke Sawa (Osaka Prefecture University)

We propose a new method to design 3-branch optical power dividers. According to the scalar Helmholtz equation, if a complex field distribution is given, then one corresponding refractive index distribution is determined uniquely. On the basis of this relationship, we first make up an ideal field which ensures smooth power division in the branching region, and next derive the refractive index distribution from this ideal field. Since the derived refractive index distribution has non-zero imaginary part and a complicated profile, it is almost impossible to fabricate the index distribution as derived. We discretize the real part into several levels and set imaginary part zero from a practical point of view. Three-branch waveguides designed by this procedure accomplish very low loss and equal division.

Keywords: optical waveguide, three-branch, equal division, low-loss, BPM

1. Introduction

Three-branch optical power dividers are one of the key elements in optical circuits. However, designing 3-branch elements is more difficult than designing Y-branch elements because we must pay attention not only to loss reduction but also to equal division. It is known that a simple fork-type 3-branch waveguide, as shown in Fig. 1, distributes more than half of the incident power to the center branch [1]. Therefore, special structures are necessary to divide optical power into three equal parts [2]~[6].

In the previous studies, 3-branch waveguides are designed on the same concept where the main attention is directed to inventing a special structure.

On the other hand, we take quite a different approach. We first consider an ideal field which propagates through the branching region losslessly. Then the refractive index distribution is derived from this ideal field by solving the Helmholtz equation inversely. Finally, low-loss 3-branch structures are realized by the practical trimming of the derived index distribution.

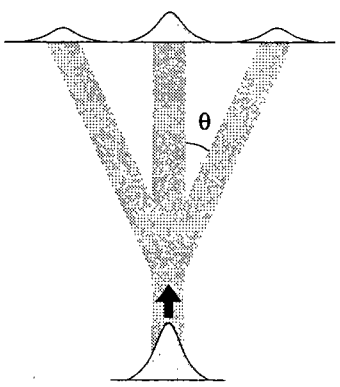

Fig. 1. Structure of simple fork-type 3-branches

2. Design method

For the sake of brevity and saving calculation time, we treat a 2-D problem. Suppose that TE waves propagate along the z direction in the slab waveguide which is uniform along the y direction. We also assume time-harmonic fields with the $e^{j\omega t}$ dependence. The complex amplitude ϕ representing E_y satisfies the following scalar Helmholtz equation.

$$\frac{\partial^2\phi}{\partial x^2}+\frac{\partial^2\phi}{\partial z^2}+k_0^2n^2\phi=0 \quad \cdots\cdots\cdots\cdots\cdots (1)$$

We consider the 3-branch waveguide as shown in Fig. 2 where the branching region is illustrated as a black box. It is assumed that we excite the dominant mode in port I. Since the input waveguide has a constant width and a constant refractive index along the z direction, the field $\phi_1(x)$ at $z=0$ also represents the dominant mode.

The complex field $\phi_2(x)$ at $z=l$ realizes the lossless equal division when it propagates toward the positive z direction. We can synthesize such a special field in the following procedure: As shown in Fig. 3(a), we inject lightwaves into ports O_1 and O_3 in phase and each port is assumed to carry one third of the power of $\phi_1(x)$. We then carry out BPM calculations toward the negative z direction. Taking complex conjugate of the resultant field at $z=l$, we obtain $\phi_2^S(x)$. Next, we inject lightwaves having the same power into port O_2 and carry out BPM calculations toward the negative z direction as shown in Fig. 3(b). Taking complex conjugate of the resultant field at $z=l$, we obtain $\phi_2^C(x)$.

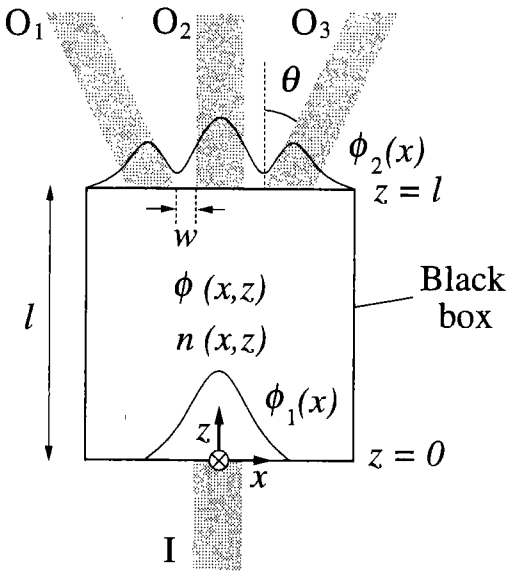

Fig. 2. Concept for 3-branches.

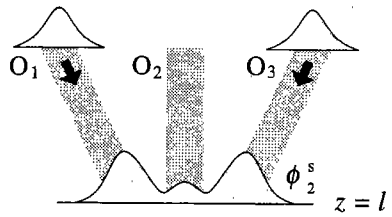

(a) Excitation of both side branches

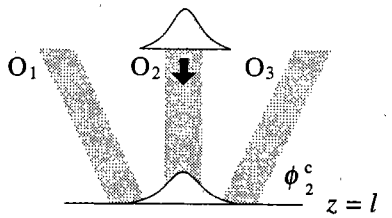

(b) Excitation to the center branch

Fig. 3. Superposition in order to make $\phi_2(x)$.

Superimposing these two fields, we obtain the field $\phi_2(x)$ as

$$\phi_2(x) = \{\phi_2^C(x) + \phi_2^S(x)\exp(j\xi)\}\exp(j\alpha) \quad \cdots (2)$$

which not only propagates toward the positive z direction losslessly but also is divided equally into ports O_1, O_2, and O_3 regardless of the values of ξ and α. This is based on the following two principles: (1) If we find out a solution of the Helmholtz equation, its complex conjugate is also a solution which expresses lightwaves propagating toward the inverse direction. (2) Because the Helmholtz equation is a linear equation, (2a) any field made by a linear combination of two solutions is also a solution; (2b) any solution multiplied by a constant is also a solution.

In the viewpoint of field, the black box in Fig. 2 is considered to be a field transformer from ϕ_1 to ϕ_2 along the distance l. Designing 3-branch waveguides is finding a realizable refractive index distribution $n(x,z)$ which accomplishes the above transformation.

Incidentally, if we solve the Helmholtz equation (1) for the refractive index distribution $n(x,z)$, then n is determined uniquely in terms of the field distribution by the following expression:

$$n = \sqrt{\frac{-1}{k_0^2\phi}\left\{\frac{\partial^2\phi}{\partial x^2} + \frac{\partial^2\phi}{\partial z^2}\right\}} \quad \cdots\cdots\cdots\cdots (3)$$

Using this principle, we propose the following design method: We first make up an ideal field distribution $\phi(x,z)$ in the black box in Fig. 2 artificially, following which the index distribution $n(x,z)$ is derived from the ideal field distribution by using (3).

For the ideal field, we assume the distribution

$$\phi(x,z) = \psi(x,z)\exp\{-jk_0n_e(z)z\} \quad \cdots\cdots\cdots (4)$$

where $\psi(x,z)$ varies moderately along the z direction while $\exp\{-jk_0n_e(z)z\}$ varies rapidly. The term $\exp\{-jk_0n_e(z)z\}$ works merely to shift the refractive index up or down as a whole along the x axis. It is $\psi(x,z)$ that yields the index variation of significance. The function $\psi(x,z)$ is constructed by interpolating $\phi_1(x)$ and $\phi_2(x)$ linearly as

$$\psi(x,z) = \{(1-a)\phi_1 + a\phi_2\}\ b(z) \quad \cdots\cdots\cdots (5)$$

where $a = z/l$. In (5), $b(z)$ is introduced to keep the power invariant along every z location. The $b(z)$ is so determined as to keep the following equation invariant:

$$P(z) \propto \int_{-\infty}^{\infty} |\ \{(1-a)\,\phi_1 + a\,\phi_2\}\ b(z)\,|^2\ dx \quad (6)$$

The linear interpolation of (5) is carried out on the complex plane. In this case, relative phase angles between $\phi_1(x)$ and $\phi_2(x)$ are of great significance. For example, if we change α in (2), the interpolation leads to a different result.

Here, we suppose the following: The phase angle of $\phi_1(x)$ has 0° anywhere on the x coordinate; the phase angles of ϕ_2^S and ϕ_2^C take 0° at $x = 0$.

In (2), there are two parameters ξ and α to adjust the phase angle of $\phi_2(x)$. For the sake of visual understanding of the parameter α, we introduce a new parameter x_p in stead of using α. The parameter x_p expresses the special point where the phase angle of $\phi_2(x)$ becomes 180°. After giving the value of ξ, we make the phase angle of ϕ_2 equal to 180° at $x = \pm x_p$ by setting α properly.

Since the phase difference between $\phi_1(x_p)$ and $\phi_2(x_p)$ is 180°, the ideal field made by interpolating ϕ_1 and ϕ_2 becomes zero somewhere on the z coordinate determined by the line $x = \pm x_p$. How to determine the value of x_p and ξ is described later.

Substituting the ideal field of (4) into (3), we obtain the refractive index distribution. If we could realize such an index distribution, lightwaves would propagate losslessly and be divided into three equal parts. However, the index distribution $n(x,z)$ obtained by (3) is almost

impossible to fabricate. The $n(x,z)$ has non-zero imaginary part which means gain or loss in the material. Gain, in particular, cannot be realized by any passive material. In addition, the spatial profile of the real part of $n(x,z)$ is very complicated.

Therefore, we must trim the index distributions obtained by (3) to make it feasible. Following two trimming schemes are necessary.

(1) imaginary part of $n(x,z)$ is set to be zero.
(2) real part of $n(x,z)$ is discretized into several values.

In practice, we employ triple-valued discretization from a fabrication viewpoint. As three values of index, we take the core index n_1, clad index n_2, and third one n_3 which is higher than the core index. We determine trimmed indices n_d having only real values by the following simple rule:

$$n_d = \begin{cases} n_1 & : \ \mathrm{Re}(n) < \dfrac{n_1+n_2}{2} \\ n_2 & : \ \dfrac{n_1+n_2}{2} \le \mathrm{Re}(n) < \dfrac{n_2+n_3}{2} \\ n_3 & : \ \dfrac{n_2+n_3}{2} \le \mathrm{Re}(n) \end{cases} \quad (7)$$

The trimming operation in (7) usually reduces the performance of the 3-branch waveguide severely. Actually, the key point of this study is how to construct the ideal field which is not severely influenced by the above trimming operation.

Suppose that the waveguide width, clad index, core index, wavelength, and branching angle θ are given. In order to minimize the influence of the trimming operation, we optimize the following factors.

(1-1) l : length of the black box in Fig. 2.
(1-2) w : space between the branches in Fig. 2.
(1-3) n_3 : value of the third refractive index for discretization in (7).
(1-4) ξ : relative phase difference between $\phi_2^C(x)$ and $\phi_2^S(x)$ in (2).
(1-5) x_p : location where the phase angle of $\phi_2(x)$ becomes 180°. This is adjusted by setting α properly in (2)
(2) $n_e(z)$: function of z in (4).

When a set of parameters l, w, n_3, ξ, and x_p is given, the function $n_e(z)$ in (4) is so determined as to minimize the following evaluating function E_1 at any z location:

$$E_1(z) = \int_{-\infty}^{\infty} [\mathrm{Re}\{n(x,z)\} - n_d(x,z)]^2 \, |\psi(x,z)| \, dx \quad (8)$$

The right-hand side of (8) expresses a sum of the square of error between the original and discretized index distributions with the ideal field as a weighting function. Decreasing values of E_1 will reduce the influence of discretization.

All of 5 parameters l, w, n_3, ξ, and x_p are so determined as to maximize the following evaluating function:

$$E_2(l,w,\xi,x_p,n_d) = \frac{\left| \int \phi_2(x) \{\phi_2'(x)\}^* dx \right|^2}{\int |\phi_2(x)|^2 dx \int |\phi_2'(x)|^2 dx} \quad (9)$$

where $\phi_2'(x)$ expresses the field obtained by the following procedure: We set the field $\phi_1(x)$ at $z=0$ and carry out BPM calculations in the black box in Fig. 2 with the index distribution derived by applying (5),(4),(3), and (7) in turn. The $\phi_2'(x)$ is the resultant field at $z=l$.

In order to evaluate E_2 once, we first solve 1-D optimization problems as many times as the longitudinal steps to obtain $n_e(z)$, and then run the BPM coding once from $z=0$ to l.

Eq. (9) expresses the correlation between $\phi_2'(x)$ and $\phi_2(x)$, which should take the maximum value when the influence of discretization of the real part and neglect of the imaginary part of the refractive index is minimized. In order to determine a set of optimum values for w, l, ξ, x_p, and n_d, we use conjugate gradient method in the 5-D searching space. Among these 5 parameters, x_p, ξ, and n_3 are more crucial than the remaining two parameters.

For saving the calculation time, it is assumed that the four parameters except w take continuous values whereas w alone takes discrete values such as $w/\lambda = 1, 2, 3, \cdots\cdots$.

3. Numerical results

3.1 Parameters fixed in numerical simulations

The parameters fixed in the following numerical simulations are as follows: The core index is 1.503, clad index 1.5, and waveguide width 4λ. This waveguide is under single-mode operation with the normalized frequency $v = 0.759\pi/2$. The index distribution in the black box in Fig.2 is given by a bitmap format whose resolution is such that $\Delta x = 0.1\lambda$ and $\Delta z = \lambda$. Therefore, $n_e(z)$ that minimizes (8) is determined at discrete points $z/\lambda = 0, 1, 2, \cdots\cdots l$ by solving a problem of minimum value searching in one dimension. Numerical simulations are carried out by FD-BPM based on the pade (1,1) approximation [7][8]. Sampling steps in FD-BPM are taken as $\Delta x = 0.1\lambda$ and $\Delta z = 1\lambda$, and the reference refractive index of BPM is set to be 1.5.

3.2 Results when the branching angle $\theta = 6°$

We show a result when the branching angle $\theta = 6°$. Maximizing the evaluating function (9), we have obtained the optimum values as $w = 1\lambda$, $l = 69\lambda$, $n_d = 1.5155$, $x_p = 6.4\lambda$, and $\xi = 73°$ by the conjugate gradient method. The value of evaluating function E_2 in (9) is 0.9811 in this case.

In the above situation, the fields $\phi_1(x)$ and $\phi_2(x)$ at the entrance and at the end of the black box, respectively, are shown in Fig.4. The solid lines express absolute values of the complex field while the broken lines express its phase angle. The gray regions express the core regions. The phase angle is expressed between $-180° \sim 180°$. In Fig. 4(b) the phase angle of $\phi_2(x)$ becomes 180° at $x = \pm 6.4\lambda (\equiv x_p)$.

Fig. 5 shows absolute values of the ideal field $\phi(x,z)$

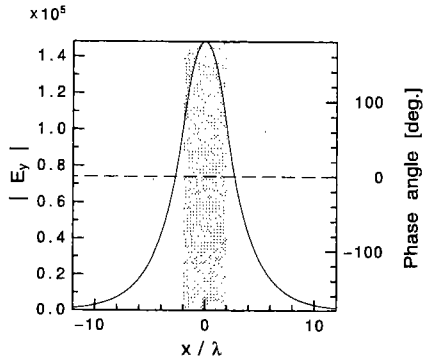

(a) $\phi_1(x)$

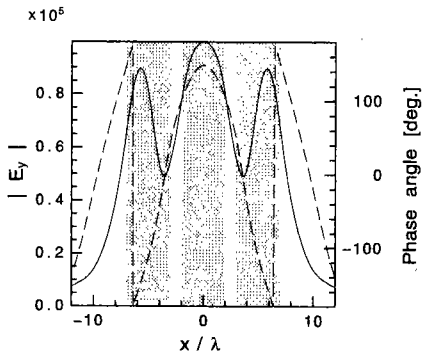

(b) $\phi_2(x)$

Fig. 4. $\phi_1(x)$ and $\phi_2(x)$ when $\theta = 6°$

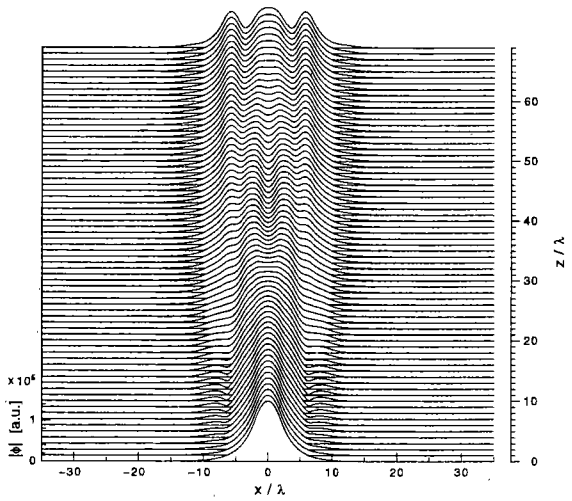

Fig. 5. Ideal field obtained by interpolation.

synthesized by (5). The absolute amplitude of the ideal field becomes zero at $x = \pm 6.4\lambda (\equiv x_p)$ and $z \simeq 10\lambda$. Substituting the ideal field into (3) and trimming the resultant index distribution by (7), we have obtained the index distribution shown in Fig. 6. The darkest region expresses the area of highest index. The value of index of this area is 1.5155 ($\equiv n_3$). In this case, $n_e(z)$ obtained has values as shown in Fig. 7.

Exciting the input port with its dominant mode, we obtain the result of BPM as shown in Fig. 8 which is expressed by absolute values of the field. There exist some differences between the ideal field of Fig. 5 and the

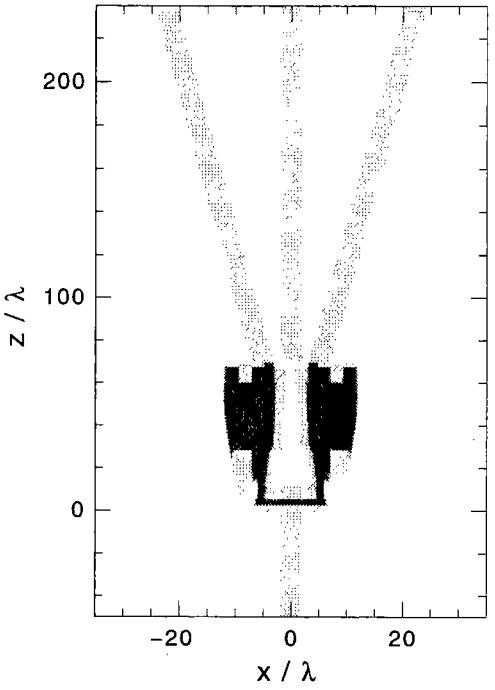

Fig. 6. Synthesized index distribution when $\theta = 6°$.

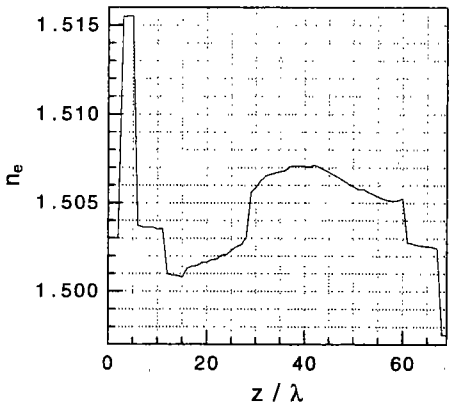

Fig. 7. Values of n_e versus z/λ

BPM results of Fig. 8 in the region $z = 0 \sim 69\lambda$. However, a value of evaluating function E_2 in (9), expressing correlation between the ideal field and BPM result at the end of the black box, is 0.9811, which is considered to be a very high score. Therefore, this structure can achive high performance with a power distribution ratio of 32.2% : 33.6% : 32.2%. The remaining 2.0% are accounted to be loss.

3.3 Numerical results when the branching angle $\theta = 4 \cdots 8°$ In the same manner, we design for the cases where the branching angle $\theta = 4, 5, 6, 7$, and 8°. Table 1 lists the optimum 5 parameters and values of evaluating function (9) at the optimum point.

The parameters shown in Table 1 give the structures shown in Fig. 9(a)~(e). The structure of Fig. 9(c) is the same that described in Fig.6.

In the case of the simple three-branch shown in Fig. 1, the length of the branching region becomes shorter as

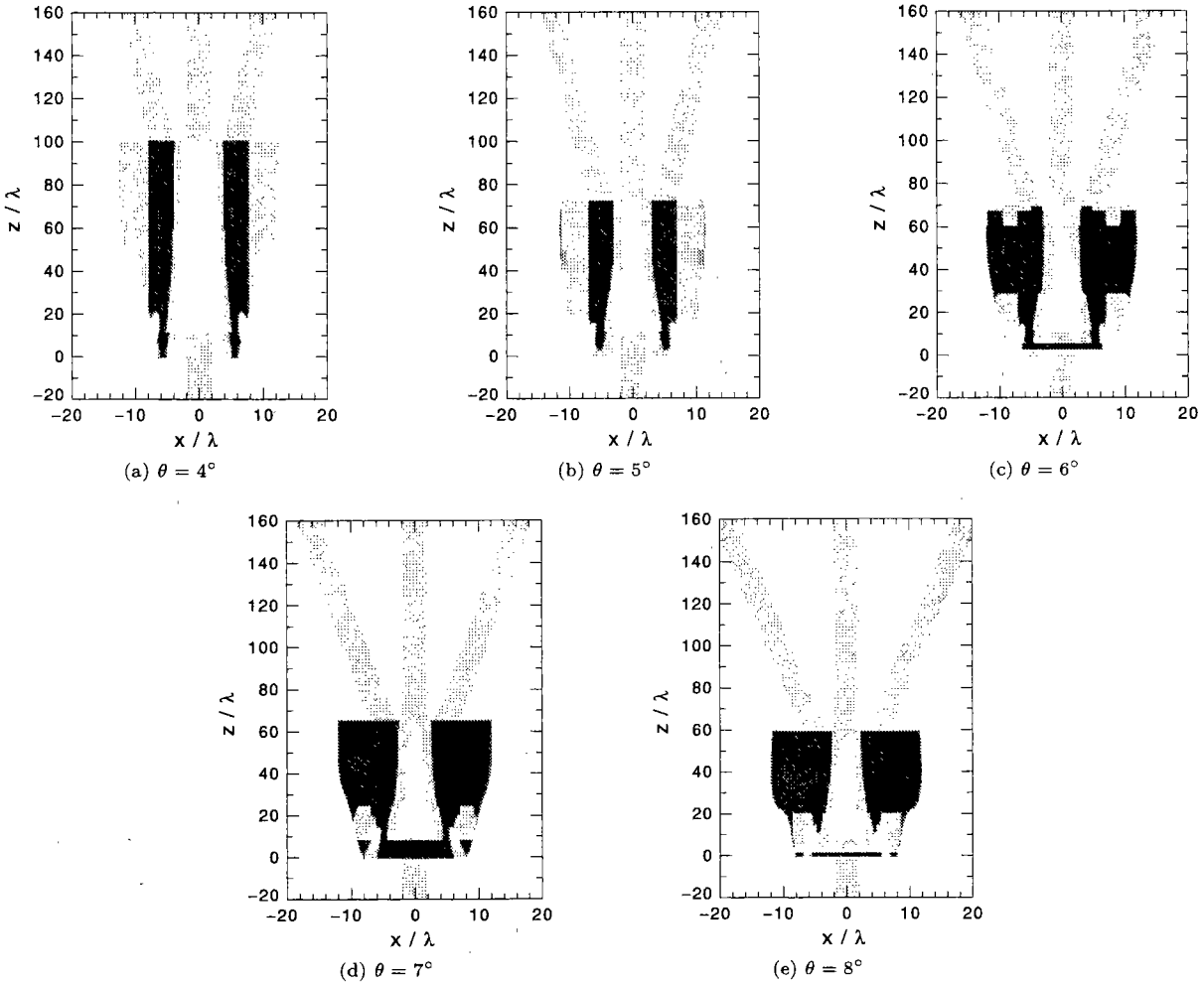

(a) $\theta = 4°$ (b) $\theta = 5°$ (c) $\theta = 6°$

(d) $\theta = 7°$ (e) $\theta = 8°$

Fig. 9. Design for the branching angle θ being $4° \sim 8°$

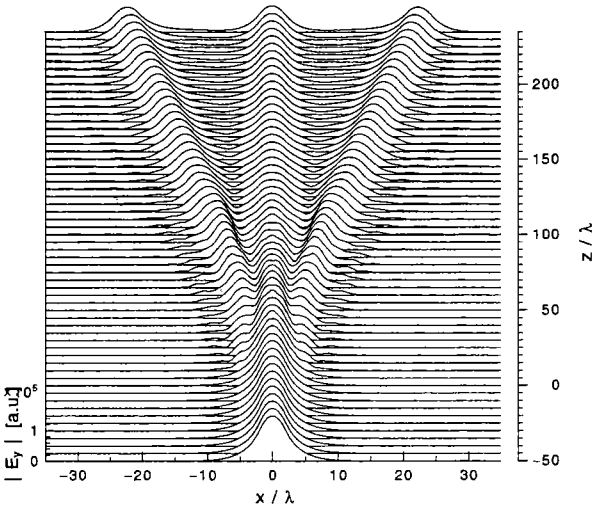

Fig. 8. Result of BPM simulation.

Table 1. Converged values of optimized 5 parameters and values of evaluating function.

θ [°]	w [λ]	l [λ]	n_3	x_p [λ]	ξ [°]	E_2 in (9)
4	2.0	100	1.5070	7.0	70	0.9949
5	1.0	72	1.5125	6.4	50	0.9802
6	1.0	69	1.5155	6.4	73	0.9811
7	1.0	65	1.5182	5.7	90	0.9694
8	1.0	59	1.5229	5.0	97	0.9598

the branching angle gets wider. This is the case with almost all branching waveguides because a wider branching angle requires that lightwaves bound to both side arms have to leave from the center axis more quickly. Our structure is not an exception at all: The wider the branches expand, the shorter the length of black box l becomes, as shown in Table 1.

In the black box, lightwaves targeting both side arms have to be turned smoothly and be injected straight to both side arms. It is expected that we need a distance somewhat longer than that of the simple three-branch for this purpose. Every value of l in Table 1 is $15\lambda \sim 25\lambda$ longer than that of the simple three-branch.

It is also observed in Table 1 that a higher contrast of refractive index is necessary as the branching angle becomes wider.

The structures shown in Figs. 9(b) and 9(c) might look somewhat different each other. However, injecting lightwaves into the input port and carrying out BPM calculations for both structures, we have very similar field distributions which concentrate tightly around the

Table 2. Power distribution ratios and losses

θ [°]	P_l [%]	P_c [%]	P_r [%]	Loss [%]
4	33.1	33.4	33.1	0.4
5	33.9	30.2	33.9	2.0
6	32.2	33.6	32.2	2.0
7	33.3	30.5	33.3	2.9
8	31.2	33.4	31.2	4.2

center axis of the black box. Hence, differences in the index distribution which lightwaves actually feel are much smaller than their appearances. Indeed, the index distributions before trimming for Figs. 9(b)and 9(c) look very similar to each other. It is considered that the index trimming has exaggerated the differences of the structures.

Above discussions suggest that the structures of Fig. 9 have the following properties in common: The center region with lowest index accelerates lightwaves while regions on both sides with the highest index retard them. These effects produce such a convex wave front at the end of the black box as shown in Fig.4(b).

For the structures in Fig. 9, we have excited the dominant mode at each input port and carried out BPM calculations. Power distribution ratios in three branches and losses are summarized in Table 2 where P_l, P_c, and P_r express the power distributed to the left, center, and right branches, respectively. The remaining is considered to be loss. For every branching angle, equal division and low loss property are realized satisfactorily.

The values of E_2 in Table 1 express the correlation at the end of the black box between an ideal field and a field obtained by a BPM calculation. As mentioned previously, lightwaves are divided into equal three parts losslessly when the evaluated value E_2 is unity. When E_2 is less than unity, Tables 1 and 2 indicate what follows:

- We have losses, the amount of which is nearly equal to $1 - E_2$.
- We have slight power imbalance in the output ports but any regularity is not recognized.

4. Summary

In order to design 3-branch optical power dividers, we have proposed a new method which have a different concept from the previous studies. Using the proposed method, we have synthesized 3-branch waveguides of low-loss and equal division.

The proposed method can be applied to the design of 3-branch waveguides having an arbitrary distribution ratio. In addition, this method have a possibility to design some other optical elements: 4-branch waveguides, asymmetric Y-branch waveguides and so on.

(Manuscript received January 26, 2001, revised July 16, 2001)

References

(1) R. A. Becker and L. M. Jonson, "Low-loss multiple-branching circuit in Ti-indiffused $LiNbO_3$ channel waveguides," Optics Lett., vol.9, no.6, pp.246–248, June 1984.

(2) W.-Y. Hung, H.-P. Chan, and P. S. Chung, "Single mode 1×3 integrated optical branching circuit design using phase-front accelerators," Electron. Lett., vol.24, no.22, pp.1365–1366, Oct. 1988.

(3) S. Banba, H. Ogawa, "Novel symmetrical three-branch optical waveguide with equal power division," IEEE Microwave & Guided Wave Lett., vol.2, no.5, pp.188–190, May 1992.

(4) H. B. Lin, Y. H. Wang and W.-S. Wang, "Singlemode 1x3 integrated optical branching circuit design using microprism," Electron. Lett., vol.30, no.5, pp.408–409, March 1994.

(5) T. Yabu, M. Geshiro, N. Minami, S. Sawa, "Symmetric three-branch optical power divider with a coupling gap," IEEE J. Lightwave Technol., vol.17, no.9, pp.1693–1699, Sept. 1999.

(6) Tzyy-Jiann Wang, Yao-Hua Wang, and Way-Seen Wang, "Single-mode 1 × 3 equal-power divider using a substrate microprism and two waveguide expanders," IEEE Photon. Tech. Lett., vol.12, no.2, Feb. 2000.

(7) Y. Chung and N. Dagli, "An assessment of finite difference beam propagation method," IEEE J. Quantum Electron., vol.26, no.8, pp.1335–1339, Aug. 1990.

(8) G. R. Hadley, "Wide-angle beam propagation using Pade approximant operators," Optics Lett., vol.17, no.20, pp.1426–1428, Oct. 1992.

Yabu Teturo (Non-member) was born in Kyoto, Japan, on May 3, 1966. He received the B.E. degree in electronic engineering from Doshisha University, Kyoto, Japan, in 1989 and M.E. degree in electrical engineering from Kyoto University, Kyoto, Japan, in 1991. He withdrew from the doctoral program in 1993 and became a Research Associate at Osaka Prefecture University. He has been engaged in research on optical waveguides. Mr. Yabu is a member of the Institute of Electronics, Information and Communication Engineers (IEICE).

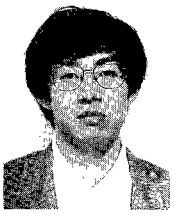

Masahiro Geshiro (Non-member) received the B.E., M.E. and Ph.D. degrees in electrical communication engineering from Osaka University, Osaka, Japan, in 1973, 1975, and 1978, respectively. From December 1979 to March 1994, he was with the Department of Electrical and Electronic Engineering, Ehime University, Matsuyama, Japan. From March 1986 to January 1987, he was a Visiting Scholar at the University of Texas at Austin, on leave from Ehime University. Since April 1994 he has been an Associate Professor of the Department of Electrical and Electronic Systems, Osaka Prefecture University, Sakai, Japan, where he is engaged in research and education on microwave engineering, optical-wave transmission lines and integrated optics. Dr. Geshiro is a member of the Institute of Electronics, Information and Communication Engineers (IEICE).

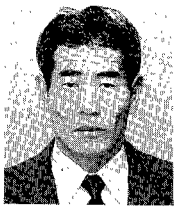

Shinnosuke Sawa (Member) was born in Osaka, Japan, on Oct. 23 in 1938. He received the B.E. degree in electrical engineering from Osaka Prefecture University, Sakai, Japan. In 1962, he joined Mitsubishi Electric Corporation, Japan, remaining there until he left in 1964. He received the M.E. and Ph.D degrees in communication engineering from Osaka University, Osaka, Japan, in 1967 and 1970, respectively. In 1970, he became an Associate Professor of Electronic Engineering, at Ehime University, Matsuyama, Japan, where he was promoted to Professor in 1976. In 1991, he became Professor in Electrical Engineering at Osaka Prefecture University, Sakai, Japan, and in 1993, Professor in Electrical and Electronic Systems. His current interests are in the area of optical waveguides, optical integrated circuits, nonlinear optics, optoelectronics, and microwave integrated circuits and components. He is a member of the Institute of Electrical and Electronics Engineers, the Institute of Electronics, Information, and Communication Engineers of Japan, the Institute of Electrical Engineers of Japan, and the Laser Society of Japan.